

Growth dynamics of untreated glioblastomas in vivo

Anne Line Stensjøen, Ole Solheim, Kjell Arne Kvistad, Asta K. Håberg, Øyvind Salvesen, and Erik Magnus Berntsen

Department of Circulation and Medical Imaging, Faculty of Medicine, Norwegian University of Science and Technology, Trondheim, Norway (A.L.S., E.M.B.); Department of Neurosurgery, St. Olavs University Hospital, Trondheim, Norway (O.S.); National Competence Centre for Ultrasound and Image Guided Therapy, St. Olavs University Hospital, Trondheim, Norway (O.S.); Department of Neuroscience, Faculty of Medicine, Norwegian University of Science and Technology, Trondheim, Norway (O.S., A.K.H.); Department of Radiology, St. Olavs University Hospital, Trondheim, Norway (K.A.K., A.K.H., E.M.B.); Department of Cancer Research and Molecular Medicine, Faculty of Medicine, Norwegian University of Science and Technology, Trondheim, Norway (Ø.S.)

Corresponding Author: Anne Line Stensjøen, Medical research student, MR Center, Department of Circulation and Medical Imaging, Faculty of Medicine, Norwegian University of Science and Technology, Post Box 8905, N-7491 Trondheim, Norway (stensjoe@stud.ntnu.no).

See the editorial by Badve and Sloan, on pages 1307–1308.

Background. Glioblastomas are primary malignant brain tumors with a dismal prognosis. Knowledge of growth rates and underlying growth dynamics is useful for understanding basic tumor biology, developing realistic tumor models, and planning treatment logistics.

Methods. By using repeated pretreatment contrast-enhanced T_1 -weighted MRI scans from 106 patients (aged 26–83 years), we studied the growth dynamics of untreated glioblastomas in vivo. Growth rates were calculated as specific growth rates and equivalent volume doubling times. The fit of different possible growth models was assessed using maximum likelihood estimations.

Results. There were large variations in growth rates between patients. The median specific growth rate of the tumors was 1.4% per day, and the equivalent volume doubling time was 49.6 days. Exploring 3 different tumor growth models showed similar statistical fit for a Gompertzian growth model and a linear radial growth model and worse fit for an exponential growth model. However, large tumors had significantly lower growth rates than smaller tumors, supporting the assumption that glioblastomas reach a plateau phase and thus exhibit Gompertzian growth.

Conclusion. Based on the fast growth rate of glioblastoma shown in this study, it is evident that poor treatment logistics will influence tumor size before surgery and can cause significant regrowth before adjuvant treatment. Since there is a known association between tumor volume, extent of surgical resection, and response to adjuvant therapy, it is likely that waiting times play a role in patient outcomes.

Keywords: brain neoplasms/pathology*, cell growth processes, glioblastoma, growth dynamics, magnetic resonance imaging.

Glioblastomas are fast-growing, malignant primary brain tumors, and the prognosis remains poor despite modern treatment regimes. Overall median survival is only 10 months for unselected patients, increasing to 16 months for patients undergoing maximal safe surgical resection followed by radiotherapy and temozolomide chemotherapy.¹

Knowledge about growth dynamics in unselected glioblastoma patients is of interest for understanding the basic biology of the disease and for developing realistic experimental tumor models. Awareness concerning the speed of growth in vivo can also be of clinical importance for patient logistics (eg, benchmarking acceptable waiting times for diagnostic work-up and treatment). However, the growth dynamics of untreated glioblastomas in vivo have not been much studied, and to our

knowledge not in large representative samples of untreated patients.

Tumor growth is the product of a complex interaction between mitotic activity, blood supply, subclonal proliferation, and cell death (ie, apoptosis or necrosis).² Considerable effort has been put into the fields of experimental and mathematical modeling of glioblastoma growth dynamics and variability,^{3,4} and several models of tumor growth have been proposed in the literature. One is simple exponential growth, in which the tumor has a constant volume-doubling time.⁵ This was first assumed for glioblastomas by Yamashita et al.⁶ Harpold et al have presented a biomathematical proliferation-invasion model of glioma growth that predicts linear growth of the radius of the tumor and describes growth rates as velocities of radial

Received 18 December 2014; accepted 6 February 2015

© The Author(s) 2015. Published by Oxford University Press on behalf of the Society for Neuro-Oncology. All rights reserved.
For permissions, please e-mail: journals.permissions@oup.com.

expansion.⁴ Gompertzian growth is perhaps one of the most acknowledged tumor growth models today.^{7–9} This model assumes initial exponential growth, but as the tumor grows the volume-doubling time increases due to lack of nutrients and subsequent cell death until growth becomes linear before finally reaching a plateau phase.⁷

Among consecutive patients scheduled for glioblastoma surgery at our institution, which serves a defined geographical catchment region, we included patients with at least 2 weeks between the diagnostic MRI and the preoperative MRI taken the day before surgery. We aimed to study the growth dynamics of untreated glioblastomas in vivo to assess speed of growth and to explore possible patterns of growth (exponential, linear radial, or Gompertzian). We also sought to assess the relationship between the contrast-enhancing part of the tumor and the central nonenhancing part in order to study any implications this has for growth dynamics.

Materials and Methods

All patients diagnosed with histopathologically verified glioblastoma at our hospital between January 2004 and May 2014 were retrospectively evaluated for inclusion. Patients eligible for inclusion were adults (aged ≥ 18 years) who underwent first-time surgery for glioblastoma, had no prior history of brain tumor, and had undergone at least 2 T₁-weighted MRI examinations with contrast before surgery. The time interval between the MRIs had to be at least 2 weeks to minimize the uncertainty in the growth rate estimates.¹⁰ Patients with noncontrast-enhancing tumors were excluded, as were patients with gliomatosis cerebri according to radiological criteria.¹¹ Furthermore, an experienced pathologist reviewed the histopathological sections of enrolled patients to ensure a uniform patient population. The study was approved by the regional ethics committee and adhered to the Helsinki Declaration.

In total, 262 glioblastoma cases were screened, of which 106 (40.8%) met the inclusion criteria. In these 106 patients, the first and last MRI scans before surgery were retrieved. The first MRI scan was performed when the patient underwent the initial diagnostic work-up (“diagnostic scan”). The last MRI scan was usually obtained the day before surgery, to be used for intraoperative neuronavigation (“preoperative scan”).

Magnetic Resonance Imaging Acquisition

The diagnostic scan was performed in one of 15 different radiology clinics, of which 12 were located in the geographical catchment region of our neurosurgical department. All preoperative scans were performed at our hospital, except for that of one patient. The contrast-enhanced T₁-weighted images from both diagnostic and preoperative examinations were used for tumor segmentation. Eight patients underwent diagnostic scanning at 1 Tesla, 85 patients at 1.5 Tesla, and 13 patients at 3 Tesla. Slice thickness varied from 0.6 to 5.0 mm, interslice gap from 0.0 to 2.0 mm, and inplane resolution from 0.4×0.4 to 1.0×1.0 mm². Preoperative scans were obtained at either 1.5 Tesla ($n = 56$) or 3 Tesla ($n = 50$) with slice thickness between 1.0 and 1.8 mm, and (with one exception) maximum 1×1 mm² in-plane resolution. High-resolution

images (defined as slice thickness ≤ 2 mm) at both scans were obtained in 61.3% of patients.

Tumor Segmentation

The software BrainVoyager QX (Brain Innovation) was used for tumor segmentation. Tumor volume was defined as the contrast-enhancing (CE) compartment of the tumor combined with the central nonenhancing (non-CE) compartment enclosed by the contrast, (the latter usually represented necrosis). In cases with multiple contrast-enhancing lesions, all lesions were segmented and included in the total tumor volume. The CE and non-CE compartments were segmented separately to allow separate investigation of growth rates (Fig. 1).

A range algorithm in the software was used to first mark all voxels with intensities above a selected threshold. Thereafter, a manual segmentation tool was used to remove voxels with high intensity due to contrast enhancement in blood vessels and meninges, followed by a manual control and delineation of the tumor border. Using the manual segmentation tool, the non-CE compartment was then segmented. Tumor volumes were calculated from the voxel volume and the number of voxels segmented. In some cases, the diagnostic images had gaps between slices, and the voxel volume was calculated as voxel-in-plane-resolution \times (slice thickness + gap thickness). The segmentations were done by the first author (A.L.S.) and verified by a radiologist (E.M.B.).

Segmentation Reproducibility

The reproducibility of the tumor segmentations was investigated using measures suggested by Bland and Altman.¹² Ten preoperative, high-resolution ($1 \times 1 \times 1$ mm³) scans from consecutive glioblastoma patients were chosen and reformatted to 5 mm slice-thickness ($1 \times 1 \times 5$ mm³). Eight of these scans had typical radiological features with a contrast-enhancing ring encapsulating a central nonenhancing area, while 2 scans had nontypical features with speckled contrast enhancement and poorly defined margins. The 8 typical glioblastomas were segmented twice by the first author (A.L.S.) using the thin slices (≤ 1.1 mm) and twice using thick slices ($= 5$ mm), with a 2-week interval between each segmentation. There was a non-significant mean difference of 0.17 mL in tumor volume between repeated segmentations on thin slices (paired samples t test, $P = .594$). The reproducibility coefficient was 1.72 mL for segmentations on thin slices; differences above this value were considered significant. There was a significant difference with a mean of 1.46 mL between tumor volumes obtained from thin and thick slices (paired samples t test, $P = .007$). The limits of agreement when comparing segmentations from thin slices with segmentations from thick slices was $1.46 \text{ mL} \pm 2.43$, and thus a difference < -0.97 mL and > 3.99 mL was considered a significant volume change.

Growth Estimations

The growth rate of individual tumors was assessed using volume doubling time (VDT), specific growth rate (SGR), and velocity of radial expansion (VRE). VDT was calculated according to the procedure of Yamashita et al.⁶ Mehrara et al suggested

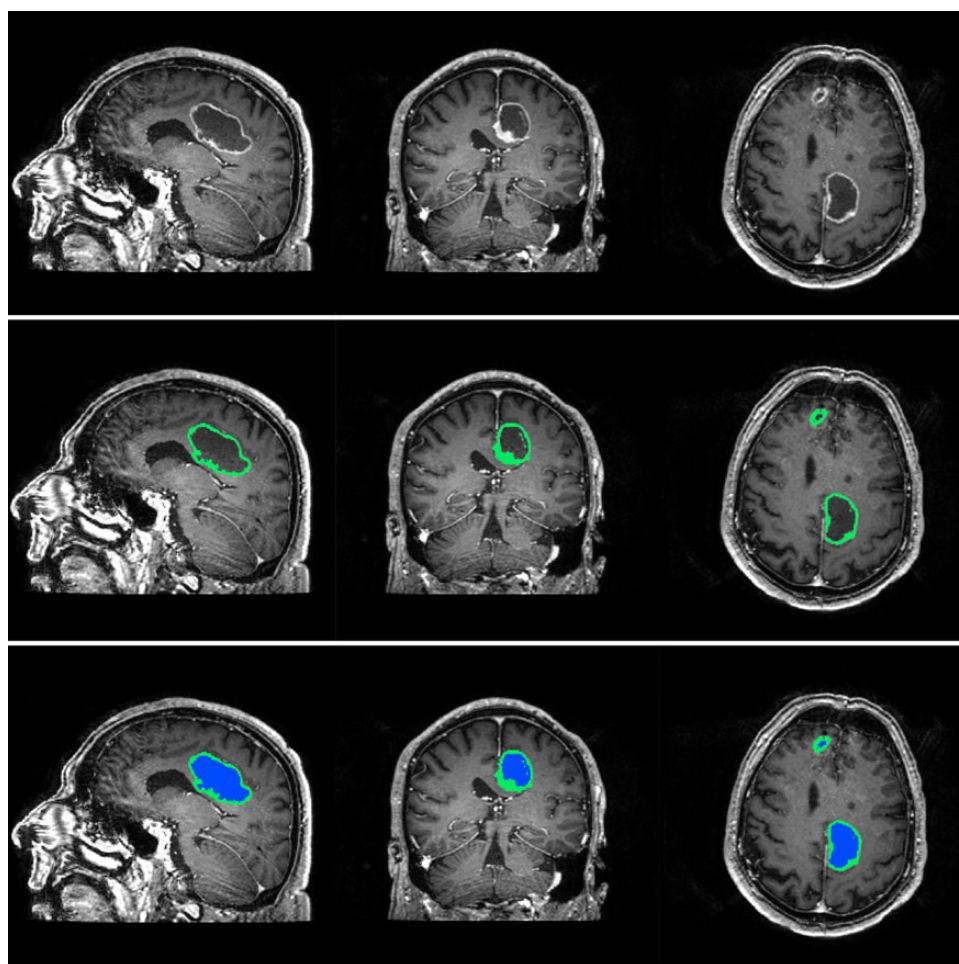


Fig. 1. Segmentation of a glioblastoma, with separate masks for contrast-enhancing and noncontrast-enhancing compartments.

that the distribution of VDT in a population tends to be skewed, thus it may be useful to transform VDT to specific growth rate, $SGR = \ln(2)/VDT$ (%/day), which is supposed to give a more symmetrical distribution.¹⁰ The median SGR can be used to calculate the equivalent VDT (eVDT) for the population, which is suggested to be a more precise estimate of the true growth rate in a population than classical median VDT. Following the procedure of Wang et al, we also calculated VRE, assuming linear growth of the radius of the tumor.¹³

Model Fitting to Data

Based on measured tumor volumes at both time points and time intervals between scans for all patients, 3 different models of tumor growth were fitted using maximum likelihood estimation (mathematical expressions are given in Table 2): (i) simple exponential growth, (ii) linear radial growth, and (iii) Gompertzian growth. The models were based on the assumptions in earlier studies of tumor growth^{6,8,13} and are explained in the online Supplementary Method. The fitting procedure gave a maximum log-likelihood for each model indicating how well the models explain the observed growth.

Statistical Analyses

The statistical significance level was set to $P < .05$. Statistical analysis was done using IBM SPSS Statistics 21.0 and R version 2.13.1. In SPSS, the explore function was used to calculate measures of central tendency and spread for each of the variables included and to assess the normality of the sample variables. To investigate if our patient sample was representative, we compared the distribution of age and sex between included and excluded patients, using the independent samples *t* test and Pearson chi-square test. The rest of the statistical tests implemented were nonparametric because the distribution of all variables was skewed, except for age. Specifically, the associations between variables were examined using Spearman correlations, and differences between groups were examined using the independent samples Mann-Whitney *U* test, the independent samples Kruskal-Wallis test, or the related samples Wilcoxon signed rank test as appropriate. For group comparisons, tumor volume was divided into 3 groups based on the 25th and 75th percentile, and pairwise comparisons were performed using Dunn's procedure¹⁴ and Bonferroni correction for multiple comparisons. SGR was used as the measure of growth in all group comparisons and correlation analyses.

Results

Patient Characteristics

Of the 106 cases included in this study, 72 were men (68%), and mean age at diagnosis was 62.9 years (range, 26–83 years). The sex and age distribution was similar among excluded patients ($P = 0.523$ and $P = 0.755$, respectively). Eighty-six (81%) of the included patients were treated with corticosteroids, while 20 patients had never received corticosteroids prior to surgery. Of the patients receiving corticosteroids, 47 (55%) were started on corticosteroids before or approximately at the same time as the first MRI, while 37 (43%) patients were given corticosteroids between the 2 MRI examinations. Two patients received corticosteroids only after both MRI examinations. The median interval between the 2 scans was 23.5 days (range, 14–98 days).

The median absolute volume change was 6.2 mL, and median relative volume change was 38.4% (Table 1). Twenty-nine tumors (27%) grew or shrunk less than the limits of agreement or reproducibility coefficient (according to our reproducibility estimates; see Materials and Methods) and were therefore regarded as having no change in volume between the 2 scans. Another 29 (27%) tumors demonstrated at least 100% volume increase between the 2 scans, while 41 (39%) tumors grew <100%. Seven (7%) tumors exhibited a negative volume change even when taking the reproducibility coefficient and limits of agreement into consideration. These tumors underwent a median volume reduction of 3.0 mL or –18.5% (Supplementary Table S1). Six of these 7 tumors had a decrease of their CE compartment, and only 2 had growth of their non-CE compartment after taking the reproducibility coefficient and limits of agreement into consideration.

Volumetric Analysis and Volume Change

The median volume of the 106 glioblastomas was 17.7 mL at the diagnostic scan and 27.5 mL at the preoperative scan.

Growth Estimates

All tumors were included in the growth rate analyses, and the median VDT was 29.8 days (Table 1). The fastest growing tumor

Table 1. Volume measures and growth rate estimates for different tumor compartments

Variable	Median (range)		
	Entire Tumor (n = 106)	Contrast Enhancement (n = 106)	Central Noncontrast-enhancing Part (n = 90)
Volume at diagnostic scan (mL)	17.7 (0.05, 146.5)	11.5 (0.05, 127.1)	5.0 (0.0, 104.6)
Volume at preoperative scan (mL)	27.5 (1.0, 243.5)	16.0 (0.9, 215.4)	10.5 (0.0, 106.5)
Absolute change (mL)	6.2 (12.8, 99.8)	3.8 (–18.6, 88.3)	2.9 (–15.6, 31.9)
Relative change (%)	38.4 (–24.9, 4808.7)	34.5 (–42.0, 3799.5)	58.5 (–89.3, 26569.1)
VDT (days)	29.8 (–7832.4, 8021.0)	27.3 (–1803.9, 5273.8)	16.7 (–875.1, 855.8)
SGR (%/day)	1.4 (–1.9, 13.2)	1.2 (–3.6, 10.7)	2.2 (–7.0, 12.6)
eVDT (days)	49.6	59.5	31.4
VRE (mm/year)	29.6 (–45.0, 212.4)	–	–

Abbreviations: eVDT, equivalent volume-doubling time; SGR, specific growth rate; VDT, volume doubling time; VRE, velocity of radial expansion.

Table 2. Growth models, parameter estimates, and log-likelihood values

Model	Mathematical Model	Statistical Model (Model Tested)	Parameter Estimates	Log-likelihood Value
Exponential growth	$V(t) = V_0 \cdot \exp(\alpha t)$	$\log V(t) = \log V_0 + \alpha t + \epsilon = \mu + \epsilon$	$\alpha = 0.01215$ $\sigma = 1.6123$	–73.135
Linear radial growth	$V(t) = (4\pi/3) \cdot (r_0 + \alpha t)^3$	$\log V(t) = \log 4\pi/3 + 3\log(r_0 + \alpha t) + \epsilon = \mu + \epsilon$	$\beta = -0.4420$ $\alpha = 0.008314$ $\sigma = 1.5037$	–54.23
Gompertzian growth	$V(t) = K \cdot \exp[\log(V_0/K) \exp(-\alpha t)]$	$\log V(t) = \log K + \log(V_0/K) \cdot \exp(-\alpha t) + \epsilon = \mu + \epsilon$	$\beta = -0.4415$ $\alpha = 0.007545$ $K = 158.04$ $\sigma = 1.5345$ $\beta = -0.4515$	–53.835

Abbreviations: K, asymptote of growth curve in Gompertz model; r_0 , radius of tumor at first scan; t, time; V, volume at second scan, V_0 , volume at first scan; α , growth parameter; β , error parameter; ϵ , random error parameter ($0, \sigma^2 \cdot e^{\beta \mu}$); μ , equations for each model.

had a VDT of 5.3 days, with a SGR of 13.2% per day. The median SGR was 1.4% (range, -1.9% to 13.2%) per day, which corresponds to an eVDT of 49.6 days. The median VRE was 29.6 mm (range, -45.0 mm to 212.4 mm) per year.

Correlation Between Tumor Growth and Tumor Size

There was a significant negative correlation between the natural logarithm of diagnostic tumor volume and SGR (Spearman $r_s(104) = -0.584$, $P < .001$) (Fig. 2). The median SGRs were significantly different between small (<3.88 mL, $n = 26$), medium (≥ 3.88 mL <36.88 mL, $n = 54$), and large tumors (≥ 36.88 mL, $n = 26$) (Kruskal-Wallis test, $P < .001$). Pairwise comparisons revealed significant differences between all 3 groups, and the small, medium, and large tumors had a median SGR of 3.9%, 1.2%, and 0.3% per day, respectively (Fig. 2, Supplementary Table S2).

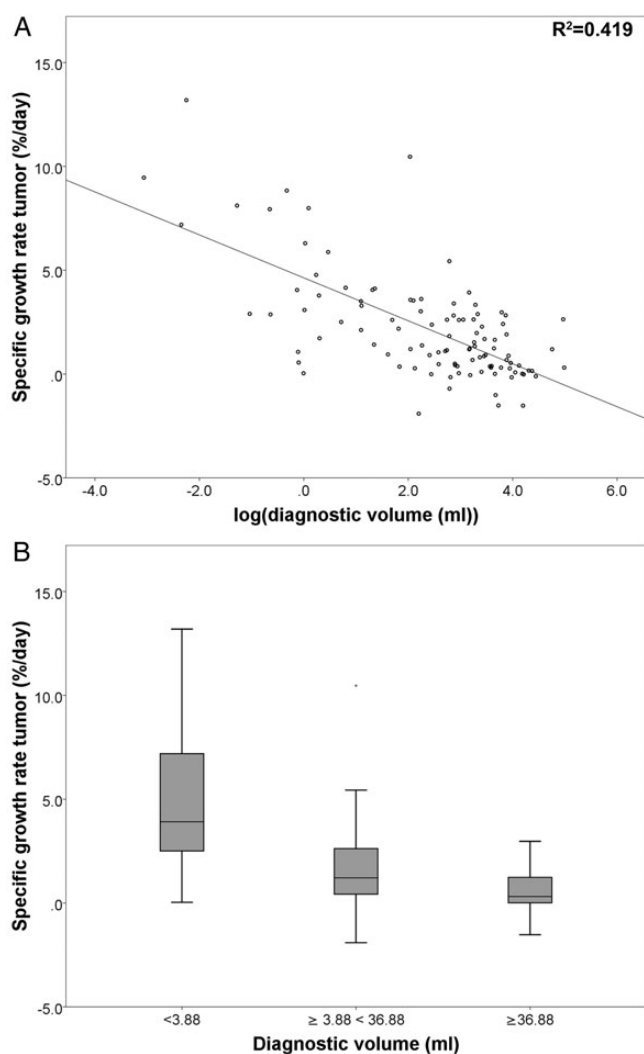


Fig. 2. Panel A shows the correlation between specific growth rate (SGR) and the natural logarithm of diagnostic tumor volume. Panel B shows differences in the distribution of SGR between tumors of different sizes ($*P < .05$).

Impact of Corticosteroid Treatment

For the 20 patients who never received corticosteroid treatment, the SGR was significantly faster than for those who received corticosteroids (median, 2.8%/day vs 1.2%/day) (Mann-Whitney U test, $P = .006$). However, patients who did not receive corticosteroid treatment had significantly smaller tumor volumes than patients who received corticosteroid treatment (median, 2.7 mL vs 20.3 mL) (Mann-Whitney U test, $P < .001$). In a linear regression model, treatment with corticosteroids was not a significant predictor of SGR after adjusting for \log_e diagnostic tumor volume ($P = .487$).

Contrast-enhancing and Non-contrast-enhancing Compartments

The median CE compartment grew from 11.5 mL to 16.0 mL between the examinations, resulting in a median SGR of 1.2% per day and median eVDT of 59.5 days (Table 1). Ninety (84.9%) tumors had a central non-CE compartment at the diagnostic scan, and these tumors had a significantly larger volume at diagnosis than the 16 tumors without a non-CE compartment (median volume, 23.7 mL vs 1.2 mL) (Mann-Whitney U test, $P < .001$). For these 90 tumors, the non-CE compartment grew significantly faster than the CE compartment (median SGR, 2.2% per day vs 1.0% per day) (Wilcoxon signed rank test, $P < .001$). Furthermore, the median relative volume of the non-CE compartment within each tumor increased significantly from 21.5% to 28.5% between the scans (Wilcoxon signed rank test, $P < .001$). For the 90 tumors with a non-CE compartment, the relative SGR of CE versus non-CE compartments was 0.61 in small tumors (<9.46 mL, $n = 22$), 0.09 in medium tumors (≥ 9.46 , <39.9 mL, $n = 46$), and -0.05 in large tumors (≥ 39.9 mL, $n = 22$) (Kruskal-Wallis test, $P = .047$). This indicates that the growth of non-CE compartments is faster relative to growth of the CE-compartments as lesions grow larger. In a post hoc linear regression analysis, the percentage of diagnostic tumor volume consisting of CE-tissue was not a predictor of tumor SGR after adjusting for total diagnostic volume ($P = .143$).

Fitting of Different Growth Models

As seen in Table 2, the maximum log-likelihood values were similar for both the Gompertzian growth model and the linear radial growth model. The simple exponential model had a lower log-likelihood than the 2 other models. Corresponding to this, the exponential model had a higher estimated standard deviation of the error term than the 2 other models. Panel A of Fig. 3 shows the fit for each of the 3 models, with predicted pre-operative volumes plotted against observed preoperative volumes. Although the exponential growth model shows worse fit, the difference of standard deviations is not readily apparent from the plots. The predicted growth curves for arbitrary tumors of different sizes under the 3 growth models are shown in panel B, illustrating the large difference between the growth curve in the exponential model and in the 2 other models, especially for small tumors.

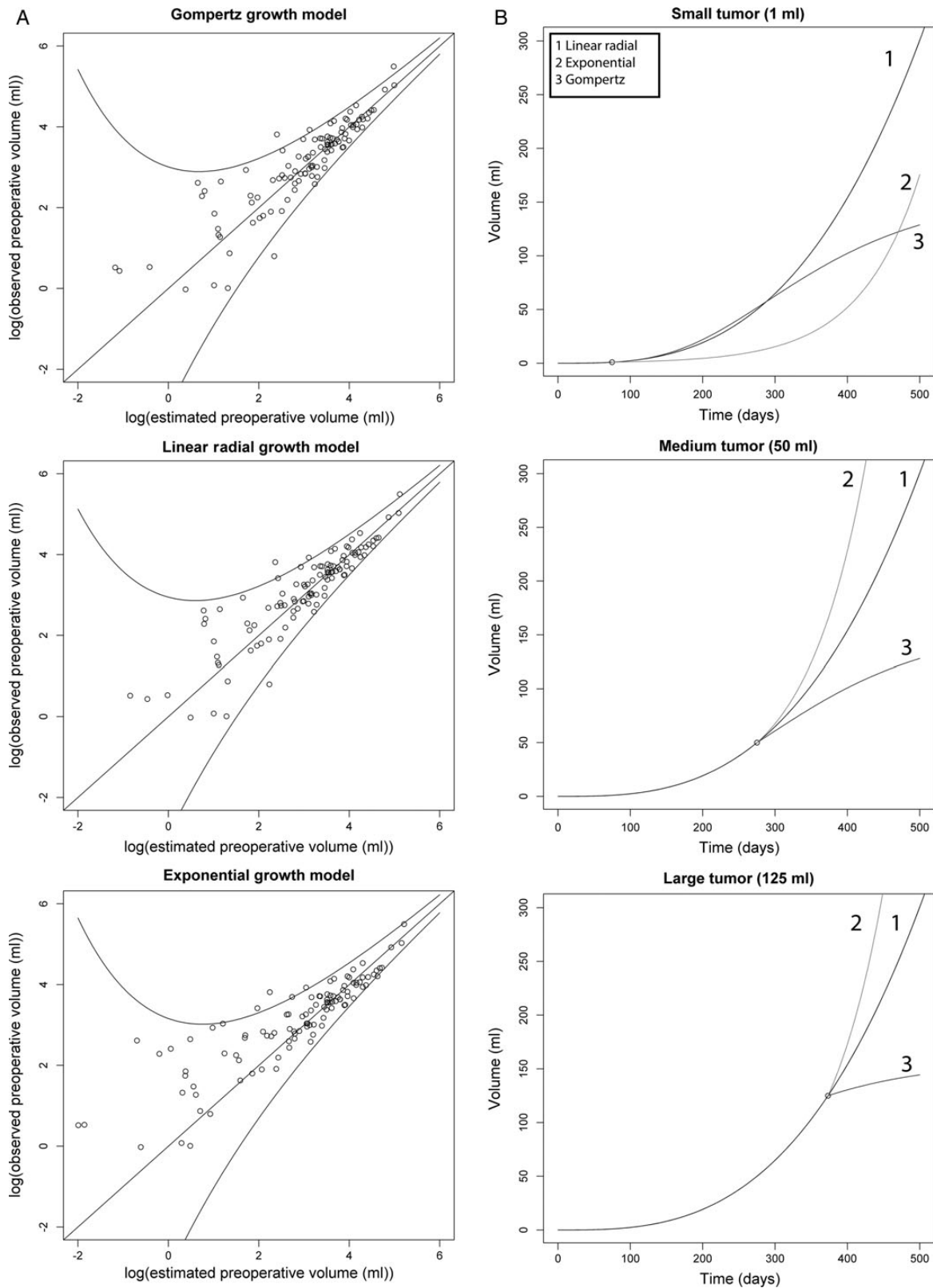


Fig. 3. Panel A shows the fit for each of the 3 models, with the natural logarithm of predicted preoperative volumes plotted against the natural logarithm of observed preoperative volumes. In a model with perfect fit, all observations would lie on the diagonal line. The outer lines represent the 95% prediction interval (ie, the interval where 95% of future observations are predicted to be found). Panel B shows predicted future growth of theoretical tumors of different sizes, in the 3 different growth models.

Discussion

We have demonstrated that glioblastomas grow very fast at the time of diagnosis but have considerable variation in growth rates between individual patients. While nearly one-third of the tumors at least doubled in volume in the period between the diagnostic scan and the preoperative scan, approximately one-third remained stable or even decreased in volume. Speed of growth in terms of SGR is much higher in smaller tumors, and the nonenhancing compartments (ie, necrotic parts of the lesions) tend to grow faster than the contrast-enhancing tissue, especially in larger tumors. Both the linear radial growth model¹³ and Gompertzian model of growth⁸ show a good fit with our data. The slower growth of large tumors indicates a plateau phase, suggesting that Gompertzian growth best describes glioblastoma growth in vivo.

Few earlier studies have explored tumor growth rates in untreated and treated glioblastoma patients (Table 3). Repeated imaging before treatment with sufficient time intervals is difficult to obtain, and posttreatment imaging studies can be difficult to interpret due to pseudoprogression,¹⁵ radiation necrosis,¹⁶ or postoperative contrast enhancement following peritumoral infarctions.¹⁷ Most earlier studies on growth of glioblastomas measured growth as VDT. The first studies were done in the 1980s on patients with recurrent gliomas, of which a few were grade IV astrocytomas. These studies used CT as the imaging modality and excluded typical glioblastomas with ring-like enhancement because of difficulties in measuring the volume.^{6,18} Later studies have measured the growth of treated glioblastomas based on either CT or MRI measurements.^{19–21} The mean VDT reported in these studies ranged from 9.7 days to 95 days as compared with a SGR of 1.4% per day, corresponding to an eVDT of 49.6 days in our study. The large variation in mean VDT in earlier studies is probably due to the small patient samples; none of the studies had more than 22 patients. Furthermore, there were substantial differences in segmentation methods and patient selection criteria. The last ten years, a few studies reporting tumor growth using other measures than VDT have been published. Pennington et al investigated the tumor growth between primary surgery and initiation of radiotherapy for 12 patients with gliomas, of which 11 were glioblastomas. They reported a median absolute tumor growth of 11.1mL (–0.02 mL to 45.1 mL) and a median relative tumor growth of 35.1% (–0.7% to 105.2%).²² This is close to the 38.4% that we found, but they had a longer scan interval with a median of 31.5 days compared with our scan interval of 23.5 days. Wang et al reported a median VRE of 30.0 mm per year (range, 3–469 mm/y) in a study on growth kinetics of 32 untreated glioblastomas.¹³ This result is very close to the median VRE of 29.6 mm per year that we found.

Seven of the tumors in our study exhibited negative growth rates, ranging down to –1.9% per day. Most previous studies only reported positive growth rates.^{6,13,18–21} Only Pennington et al reported finding a single tumor with a negative relative volume change of –0.7%.²² They made no further comment on the volume reduction. One possible explanation for the negative volume change in our 7 patients may be that these patients received corticosteroids during the interval between scans. The use of corticosteroids has previously been associated with significantly decreased tumor volumes in a study on

Table 3. Previous studies reporting growth rates of glioblastomas

Authors	Year	Included Patients	Number of Patients	Measure of Growth	Value (mean/median) (range)	Imaging Modality	What They Segmented
Yamashita ⁶	1983	Relapse tumors	6	Doubling time (days)	19.3 ± 2.1 ^a (15.0–21.0)	CT	Contrast enhancement
Tsuboi ¹⁸	1986	Relapse tumors	14	Doubling time (days)	46.8 ± 19.0 ^a (21.2–83.2)	CT	Contrast enhancement
Blankenberg ¹⁹	1995	Residual tumor after treatment or recurrent tumor	8	Doubling time (days)	96.0 ± 57.8 ^a (22–181)	MRI and CT	Contrast enhancement
Haney ²⁰	2001	GBM patients during treatment	10	Doubling time (days)	9.7 ± 99.8 (not stated)	MRI	Contrast enhancement
Pennington ²²	2006	Residual tumor after surgery, before radiation	12	Relative growth (%)	35 (–0.67–105.2)	MRI	Contrast enhancement, necrotic and cystic areas
James ²¹	2007	Patients with tumors not available for surgery	22	Doubling time (days)	95 (1.4–319)	CT	Not stated
Wang ¹³	2009	GBM patients prior to surgery	32	Velocity of radial expansion (mm/y)	30 ^a (3–469)	MRI	Contrast enhancement, including any central necrosis

^aValues calculated from table in article.

recurrent malignant gliomas, but these patients had previously been treated with radiotherapy and adjuvant chemotherapy.²³ It is therefore uncertain if the volume reduction in that sample represented reduction of the true tumor volume or of treatment-associated contrast enhancement.¹⁵ Still, cases of previously untreated glioblastomas with pseudoresponse after corticosteroid administration, both on CT and MRI images, have been reported.^{24,25} All patients with shrinking tumors in our study had received corticosteroids some time before the second MRI scan, but so had 81% of all patients included (and in similar doses). Four patients with shrinking tumors were started on corticosteroids between the first and the second scan, while 3 received corticosteroids before the first MRI scan. Furthermore, we did not find that treatment with corticosteroids was a significant predictor of SGR. Another possible reason for 5 of the 7 shrinking tumors might be low-resolution diagnostic scans and high-resolution preoperative scans, which could theoretically lead to overestimation of the diagnostic volume (ie, partial volume effect).²⁶ We did find a small overestimation of the tumor volume using thick slices compared with thin slices when we investigated the reproducibility of our segmentations. However, we did attempt to correct for this difference by using the limits of agreement to determine which tumors had a significant volume change. Six of these 7 tumors exhibited a decrease of their CE compartment, and only 2 had growth of their non-CE compartment (taking the reproducibility coefficients and limits of agreement into consideration). This could indicate a collapse due to necrosis as the reason for decreasing tumor volume in some of these patients. In summary, tumor shrinkage was present in a small subgroup, and could be partly due to tumor biology and partly related to methodological issues in our study.

We also addressed the question of the overall growth pattern of glioblastomas. Using maximum likelihood estimations, we tested 3 candidate models previously reported in the literature (namely exponential,⁶ linear radial¹³ and Gompertzian growth).⁸ However, we cannot draw firm conclusions about the true dynamics of glioblastoma growth because we lacked sufficient measurement points for each tumor. By assessing the fit for the different models, we found that the Gompertzian model and linear radial growth model had log-likelihood values in the same range. The exponential model had a lower log-likelihood value, which indicates worse fit and more uncertainty in estimates based on this model. For small tumor volumes, the future growth predicted by the Gompertz curve and the linear radial growth curve were somewhat similar (Fig. 3B). The predicted exponential growth curve is very different from the 2 other curves, and the worse fit of the exponential model might indicate that the true growth curve of glioblastomas lies closer to the 2 other curves. While the Gompertzian growth model reached an asymptote for large tumors where the growth rate was zero, this was not true for the other two models. This means, for large tumor volumes, that there was a major difference between the predicted values obtained with the 3 models. Unfortunately, we had too few large tumors to be able to differentiate between the fit of the Gompertzian model and the linear radial growth model in the range of tumor volumes, where the two models differed most. However, we found a significantly slower growth rate of the largest tumors compared with small and medium-sized

tumors. This indicates that large tumors reach a plateau with slower growth rates, in agreement with the Gompertzian growth model.⁸

We also found a significantly faster growth of the non-CE compartment compared with the CE, and a corresponding significant increase in the relative volume of the non-CE compartment within each tumor at the preoperative scan. The central non-CE compartment of glioblastomas generally consists of necrotized tumor tissue, and an increasing percentage of necrosis in the tumors might indicate that the tumors outgrow their supply of nutrition. The growth rate of the non-CE compartments was relatively higher than the growth rate of CE-compartments as lesions grew larger, illustrating the plateau phase of Gompertzian growth curve that may result from lack of nutrients and necrosis.

The impact of patient logistics (ie, waiting times) on treatment of glioblastoma patients remains controversial. There are no randomized trials, and there is conflicting evidence from rather heterogeneous observational studies.²⁷⁻³⁰ However, studying the impact of waiting times in retrospective case series can be biased because delays may occur for a reason. One example may be delays due to revisions and second opinions of initial histopathological samples in cases of very small lesions with limited tissue, or atypical presentation or in transformed low-grade gliomas that are associated with a better prognosis than primary glioblastomas. Based on our results, it seems evident that poor logistics will have effects on the tumor size preoperatively. Since there is a known association between preoperative tumor volumes and extent of surgical resection,³¹⁻³³ and since residual tumor volume and extent of resection are associated with survival,³²⁻³⁵ it is likely that patient logistics, both in terms of waiting times for surgery and waiting times for postoperative radiotherapy, play a role in patient outcome.

The untreated glioblastomas in the present study grew 6.2 mL while waiting 23.5 days for surgery. In comparison, in the 2 randomized trials that compared tools for increasing the extent of resection in glioblastoma (namely fluorescence-guided surgery with 5-ALA and high-field intraoperative MRI), the differences in median residual tumor volumes between the intervention groups and controls were only 0.7 mL and 0.03 mL, respectively.^{36,37} Although there can be apparent gains with modern surgical tools, it seems clear that the clinical advantage associated with removing such small additional tumor volumes could easily be lost due to poor treatment logistics, (ie, long waiting times before surgery and before adjuvant treatment). When a tumor is resected sooner rather than later, there is a greater chance for better surgical results and less chance for involving eloquent structures. With a daily growth of 1.4% and doubling of volume in 50 days, diagnostic work-ups, surgery, and adjuvant treatment should not be delayed if optimal treatment is to be achieved.

Strengths and Limitations

A major strength of the present study is the large and representative patient sample from one neurosurgical center with a population-based referral. Neither age nor sex distributions differed significantly between included and excluded patients, and the mean age was comparable to glioblastoma patients

in Norway.³⁸ Another major strength, compared with earlier studies, is that none of the patients received any intervention other than symptomatic corticosteroid treatment in the interval between the 2 scans, enabling us to study the growth dynamics of untreated glioblastoma in vivo. As stated earlier, the administration of corticosteroids did not seem to have a large effect on our results, and withholding symptomatic treatment is not feasible in any human study setting.

This is also the first study to investigate the growth of CE and central non-CE compartments separately. We used manual segmentation (the gold standard for tumor segmentation) to obtain volume estimates that were as accurate as possible.³⁹ Since 61.3% of the patients had high resolution MRIs both diagnostically and preoperatively, their tumor segmentation could be controlled in all orthogonal planes. The large variation in diagnostic MRI scanners and imaging parameters represents a potential source of error, which we attempted to prevent by assessing the reproducibility of our segmentations. Tumor segmentations were also verified by a radiologist, which can be expected to increase their reproducibility. The significant difference we found between volumes obtained with thin and thick slices indicates a slight overestimation of tumor volume in the thick slices, which could mean that we made a slight underestimation in the growth rate for 38.7% of our patients, including 5 of the shrinking tumors. Still, we found low reproducibility coefficients and narrow limits of agreement, indicating that our estimates of tumor growth were good.

We only assessed the growth of tumor volume as depicted on contrast enhanced T₁-weighted images. The amount of contrast enhancement on pretreatment MRI does not rely solely on tumor activity but instead may be affected by factors such as the amount and timing of contrast agent and coexisting factors such as infarctions.⁴⁰ It is also known that tumor cells migrate far outside the border of the tumors as seen on structural MRI,⁴¹ but we still used this as a measure of bulk tumor volume because the contrast-enhanced T₁-weighted image is the basis for both the evaluation of resection grade and the assessment of treatment response of enhancing gliomas.^{35,42}

We had to make different assumptions to obtain estimates of growth rates in this study. First, in line with previous studies, we assumed that the tumors exhibited a constant growth rate during the measurement interval. Assuming exponential growth during the measurement interval will probably yield an overestimated growth rate for large tumors. Nevertheless, we think that volume doubling time, or the logarithmic transformation, specific growth rate, could be used as a point measure of glioblastoma growth because these intuitive measures are easy to relate to in a clinical setting. Using volume-doubling time also allowed us to look at the growth of tumor volume with no assumptions about the shape of the tumors. This strategy is particularly useful for glioblastomas because they are highly irregular tumors that seldom resemble spheres. We also estimated the velocity of radial expansion of the tumors to compare our results with the only other study that reported growth rates of untreated glioblastomas.¹³ To obtain this measure, we used the tumor volume to calculate a spherically equivalent radius, which was then assumed to follow linear growth over time. This conversion to radial growth is rather difficult to relate to the complex shape of glioblastomas observed in clinical practice.

Conclusion

Our study clearly underlines the rapid growth rate of many glioblastomas in vivo as we found a daily growth of 1.4% and an equivalent volume doubling time of 49.6 days. However, there were large variations between individual patients. Nearly one-third of the tumors had more than doubled in volume in the waiting period between the diagnostic and preoperative scans, and approximately one-third were practically unchanged or even decreased in volume. Fitting of the different growth models showed similar statistical fit for the Gompertzian growth model and the linear radial growth model. However, large tumors demonstrated much slower growth than small tumors, giving further support to the assumption that glioblastomas exhibit Gompertzian growth.

Supplementary Material

Supplementary material is available at *Neuro-Oncology Journal* online (<http://neuro-oncology.oxfordjournals.org/>).

Funding

Anne Line Stensjøen has received a research scholarship from the Norwegian University of Science and Technology. Ole Solheim has received a salary as a researcher from the National Competence Centre for Ultrasound and Image Guided Therapy. Erik M. Berntsen and Asta K. Håberg have received salaries as researchers from the Norwegian National Advisory Unit on Functional MRI Methods.

Acknowledgments

We would like to thank Professor Sverre Helge Torp for the histopathological review of the glioblastoma diagnosis in all included patients.

Conflict of interest statement. Ole Solheim and Kjell Arne Kvistad are both unpaid members of a national advisory committee on treatment guidelines for brain tumors. The other authors disclose no potential conflicts of interest.

References

1. Ronning PA, Helseth E, Meling TR, et al. A population-based study on the effect of temozolomide in the treatment of glioblastoma multiforme. *Neuro Oncol.* 2012;14(9):1178–1184.
2. Stricker TP, Kumar V. Neoplasia. In: Kumar V, Abbas Fausto AKN, Aster JC, eds. *Robbins and Cotran Pathologic Basis of Disease*. 8th ed. Philadelphia: Elsevier Health Sciences; 2010:259–330.
3. Massey SC, Assanah MC, Lopez KA, et al. Glial progenitor cell recruitment drives aggressive glioma growth: mathematical and experimental modelling. *J R Soc Interface.* 2012;9(73):1757–1766.
4. Harpold HL, Alvord EC Jr., Swanson KR. The evolution of mathematical modeling of glioma proliferation and invasion. *J Neuropathol Exp Neurol.* 2007;66(1):1–9.
5. Schwartz M. A biomathematical approach to clinical tumor growth. *Cancer.* 1961;14:1272–1294.

6. Yamashita T, Kuwabara T. Estimation of rate of growth of malignant brain tumors by computed tomography scanning. *Surg Neurol.* 1983;20(6):464–470.
7. Laird AK. Dynamics of tumor growth. *Br J Cancer.* 1964;13:490–502.
8. Chignola R, Foroni RI. Estimating the growth kinetics of experimental tumors from as few as two determinations of tumor size: implications for clinical oncology. *IEEE Trans Biomed Eng.* 2005;52(5):808–815.
9. Nakasu S, Nakasu Y, Fukami T, et al. Growth curve analysis of asymptomatic and symptomatic meningiomas. *J Neurooncol.* 2011;102(2):303–310.
10. Mehrara E, Forsell-Aronsson E, Ahlman H, et al. Specific growth rate versus doubling time for quantitative characterization of tumor growth rate. *Cancer Res.* 2007;67(8):3970–3975.
11. Osborn AG. Astrocytomas. In: Osborn AG, ed. *Osborn's Brain: Imaging, Pathology, and Anatomy.* Salt Lake City: Amirsys, Inc; 2012; 435–472.
12. Bland JM, Altman DG. Statistical methods for assessing agreement between two methods of clinical measurement. *Lancet.* 1986;1(8476):307–310.
13. Wang CH, Rockhill JK, Mrugala M, et al. Prognostic significance of growth kinetics in newly diagnosed glioblastomas revealed by combining serial imaging with a novel biomathematical model. *Cancer Res.* 2009;69(23):9133–9140.
14. Dunn OJ. Multiple Comparisons Using Rank Sums. *Technometrics.* 1964;6(3):241–252.
15. Brandsma D, Stalpers L, Taal W, et al. Clinical features, mechanisms, and management of pseudoprogression in malignant gliomas. *Lancet Oncol.* 2008;9(5):453–461.
16. Kumar AJ, Leeds NE, Fuller GN, et al. Malignant gliomas: MR imaging spectrum of radiation therapy- and chemotherapy-induced necrosis of the brain after treatment. *Radiology.* 2000;217(2):377–384.
17. Ulmer S, Braga TA, Barker FG 2nd, et al. Clinical and radiographic features of peritumoral infarction following resection of glioblastoma. *Neurology.* 2006;67(9):1668–1670.
18. Tsuboi K, Yoshii Y, Nakagawa K, et al. Regrowth patterns of supratentorial gliomas: estimation from computed tomographic scans. *Neurosurgery.* 1986;19(6):946–951.
19. Blankenberg FG, Teplitz RL, Ellis W, et al. The influence of volumetric tumor doubling time, DNA ploidy, and histologic grade on the survival of patients with intracranial astrocytomas. *AJNR Am J Neuroradiol.* 1995;16(5):1001–1012.
20. Haney SM, Thompson PM, Cloughesy TF, et al. Tracking tumor growth rates in patients with malignant gliomas: a test of two algorithms. *AJNR Am J Neuroradiol.* 2001;22(1):73–82.
21. James BM, Gillard JH, Antoun NM, et al. Glioblastoma doubling time and cellular proliferation markers. *Clin Oncol (R Coll Radiol).* 2007;19(3):S33.
22. Pennington C, Kilbride L, Grant R, et al. A pilot study of brain tumour growth between radiotherapy planning and delivery. *Clin Oncol (R Coll Radiol).* 2006;18(2):104–108.
23. Watling CJ, Lee DH, Macdonald DR, et al. Corticosteroid-induced magnetic resonance imaging changes in patients with recurrent malignant glioma. *J Clin Oncol.* 1994;12(9):1886–1889.
24. Mazur MD, Nguyen V, Fufts DW. Glioblastoma presenting with steroid-induced pseudoregression of contrast enhancement on magnetic resonance imaging. *Case Rep Neurol Med.* 2012;2012:6.
25. Hasegawa H, Pal D, Ramirez R, et al. Glioblastoma multiforme fades on CT imaging after dexamethasone therapy. *J Clin Neurosci.* 2009;16(12):1707–1708.
26. Galloway RL Jr., Maciunas RJ, Failing AL. Factors affecting perceived tumor volumes in magnetic resonance imaging. *Ann Biomed Eng.* 1993;21(4):367–375.
27. Noel G, Huchet A, Feuvret L, et al. Waiting times before initiation of radiotherapy might not affect outcomes for patients with glioblastoma: a French retrospective analysis of patients treated in the era of concomitant temozolomide and radiotherapy. *J Neurooncol.* 2012;109(1):167–175.
28. Glinski B, Urbanski J, Hetnal M, et al. Prognostic value of the interval from surgery to initiation of radiation therapy in correlation with some histo-clinical parameters in patients with malignant supratentorial gliomas. *Contemp Oncol (Pozn).* 2012;16(1):34–37.
29. Lawrence YR, Blumenthal DT, Matcayevsky D, et al. Delayed initiation of radiotherapy for glioblastoma: how important is it to push to the front (or the back) of the line? *J Neurooncol.* 2011;105(1):1–7.
30. Spratt DE, Folkert M, Zumsteg ZS, et al. Temporal relationship of post-operative radiotherapy with temozolomide and oncologic outcome for glioblastoma. *J Neurooncol.* 2014;116(2):357–363.
31. Solheim O, Selbekk T, Jakola AS, et al. Ultrasound-guided operations in unselected high-grade gliomas--overall results, impact of image quality and patient selection. *Acta Neurochir (Wien).* 2010;152(11):1873–1886.
32. Grabowski MM, Recinos PF, Nowacki AS, et al. Residual tumor volume versus extent of resection: predictors of survival after surgery for glioblastoma. *J Neurosurg.* 2014;121(5):1115–1123.
33. Sanai N, Polley MY, McDermott MW, et al. An extent of resection threshold for newly diagnosed glioblastomas. *J Neurosurg.* 2011;115(1):3–8.
34. Solheim O, Gulati S, Jakola AS. Glioblastoma resection: in search of a threshold between worthwhile and futile. *Neuro Oncol.* 2014;16(4):610–611.
35. Lacroix M, Abi-Said D, Fourney DR, et al. A multivariate analysis of 416 patients with glioblastoma multiforme: prognosis, extent of resection, and survival. *J Neurosurg.* 2001;95(2):190–198.
36. Stummer W, Pichlmeier U, Meinel T, et al. Fluorescence-guided surgery with 5-aminolevulinic acid for resection of malignant glioma: a randomised controlled multicentre phase III trial. *Lancet Oncol.* 2006;7(5):392–401.
37. Senft C, Bink A, Franz K, et al. Intraoperative MRI guidance and extent of resection in glioma surgery: a randomised, controlled trial. *Lancet Oncol.* 2011;12(11):997–1003.
38. Storstein A, Helseth E, Johannesen TB, et al. Høygradige gliomer hos voksne. *Tidsskr Nor Laegeforen.* 2011;131(3):238–241.
39. Bauer S, Wiest R, Nolte PL, et al. A survey of MRI-based medical image analysis for brain tumor studies. *Phys Med Biol.* 2013;58(13):R97–R129.
40. Quant EC, Wen PY. Response assessment in neuro-oncology. *Curr Oncol Rep.* 2011;13(1):50–56.
41. Kelly PJ, Dumas-Duport C, Kispert DB, et al. Imaging-based stereotaxic serial biopsies in untreated intracranial glial neoplasms. *J Neurosurg.* 1987;66(6):865–874.
42. Wen PY, Macdonald DR, Reardon DA, et al. Updated response assessment criteria for high-grade gliomas: response assessment in neuro-oncology working group. *J Clin Oncol.* 2010;28(11):1963–1972.